Research Article | Vol. 28, No. 4 / 17 February 2020 / Optics Express 5629
Optics EXPRESS

Anisotropic photoluminescence of nonpolar ZnO epilayers and ZnO/$Zn_{1-x}Mg_xO$ multiple quantum wells grown on $LiGaO_2$ substrate

Tao Yan,[1,2] L. Trinkler,[3] V. Korsaks,[3] C.-Y. J. Lu,[1] B. Berzina,[3] L. Chang,[1,*] M. M. C. Chou,[1] and K. H. Ploog[1]

[1]*Department of Materials and Optoelectronic Science, National Sun Yat-sen University, Kaohsiung 80424, Taiwan*
[2]*Key Laboratory of Optoelectronic Materials Chemistry and Physics, Fujian Institute of Research on the Structure of Matter, Chinese Academy of Sciences, Fuzhou 350002, China*
[3]*Institute of Solid State Physics, University of Latvia, Kengaraga 8, 1063 Riga, Latvia*
[*]*lwchang@mail.nsysu.edu.tw*

Abstract: The temperature-dependent polarized photoluminescence spectra of nonpolar ZnO samples were investigated by 263 nm laser. The degree of polarization (DOP) of m-plane quantum wells changes from 76% at 10 K to 40% at 300 K, which is much higher than that of epilayer. The strong anisotropy was presumably attributed to the enhanced confinement effect of a one-dimension confinement structure formed by the intersection of quantum well and basal stacking fault. The polarization of laser beam also has an influence on the DOP. It is assumed that the luminescence polarization should be affected not only by the in-plane strains but also the microstructural defects, which do modify the electronic band structure.

1. Introduction

Nonpolar ZnO heterostructures exhibit two major advantages. First, the heterostructures are free from the spontaneous polarization fields in the growth direction. The quantum confined Stark effect and the associated red shift of the near band-edge emission can be avoided [1–4]. Second, the heterostructures exhibit intrinsically an in-plane optical anisotropy according to the polarization selection rules [5–7]. Due to these two characteristics, light emitting devices fabricated from nonpolar ZnO heterostructures can find unique applications such as the back light for liquid crystal displays [8,9]. In addition, the optical anisotropy can be utilized in polarized light emission [10], polarization sensitive photodetector [11], converter in optical communication [12], nonlinear optical component [13], and gas sensing [14]. For example, the maximum responsivity at light polarized perpendicular to *c*-axis of a-plane ZnO/ZnMgO quantum wells (QWs) was found to be about 5 times that of parallel to *c*-axis [11]. The relationship between the degree of polarization (DOP) and the device performance is, however, seldom reported.

The DOP for luminescence of nonpolar ZnO was, however, affected strongly by the magnitude and direction of the in-plane strains [7–9,15]. The polarization was improved with the compressive lattice strains in a-plane [2,5] and m-plane ZnO [8] compared to a strain-free layer. On the contrary, the large DOP was ascribed to the small in-plane strains [16] or enhanced strain relaxation [7] in a-plane ZnO. It is interesting that the tensile strain leads to an abnormally low polarization in m-plane ZnO [9]. Except for the lattice strain, large polarization was also attributed to the small striped domain structure in a-plane ZnO grown at low temperature [17]. Moreover, the DOP at low temperature is generally larger than that at room temperature [4,8,15], though a homoepitaxial a-plane QW showed that its polarization is independent of temperature [3].

#385828 https://doi.org/10.1364/OE.385828
Journal © 2020 Received 16 Dec 2019; revised 2 Feb 2020; accepted 3 Feb 2020; published 13 Feb 2020

Optics EXPRESS

Many nonpolar ZnO epilayers exhibited a common microstructural feature of high density of basal stacking faults (BSFs), as compared to their polar counterparts [18–21]. The unique arrangement of the close-packed plane of type I_1 BSF transforms itself to a three-layered zincblende structure. This three-layered structure is also treated as a type II QW in which the optical transition is allowed. Optical emission from BSFs at low temperature has widely been reported from photoluminescence (PL) and cathodoluminescence (CL) results. In addition, the evidence from CL spectroscopy demonstrates that the emission from BSF is not quenched but turns broad at room temperature [20]. It has been proposed that the intersection of QW and BSF forms a quantum line (QL) state which should be highly anisotropic in optical emission [4]. Since the anisotropy is originated from a geometrical effect instead of a crystal symmetrical effect, the polarization resulted from the QLs should not be affected by the in-plane strain state.

$LiGaO_2$ (LGO) (100) and (010) substrates have been demonstrated to be suitable for growing nonpolar m- and a-plane ZnO epilayers, respectively [22–24]. The lattice mismatch is 1.9% in $[11\bar{2}0]$ZnO//[010]LGO, 3.9% in [0001]ZnO//[001]LGO, and 4.1% in $[10\bar{1}0]$ZnO//[100]LGO, all of which will further decrease at the actual growth temperature of 700 °C due to thermal expansion. The epilayers grown on LGO (100) and (010) substrates have different strain states, and the effect of strain on the polarization anisotropy can be studied.

In this work, nonpolar m- and a-plane ZnO epilayers and $ZnO/Zn_{1-x}Mg_xO$ multiple QWs have been grown on LGO substrates by plasma-assisted molecular beam epitaxy (MBE). The polarized PL spectra at different temperatures were measured systematically in order to investigate the anisotropic emission characteristics.

2. Experiment

The samples were grown on LGO substrates in a CreaTec SY094 system equipped with a radio frequency oxygen plasma source and two effusion cells for elemental Zn and Mg. The growth of ZnO epilayers and QWs was carried out at 700 °C at oxygen pressure of 5×10^{-6} mbar with the plasma power of 300 W. The thickness of m- and a-plane ZnO epilayers was determined to be about 300 and 150 nm from cross-section scanning electron microscopy (SEM) images. For the growth of m-plane ZnO QWs, a ZnO buffer layer of 30 nm was deposited on the substrate in order to smoothen the surface as observed by reflection high energy electron diffraction (RHEED). Then a layer of 40 nm $Zn_{0.55}Mg_{0.45}O$ was grown at a Zn/Mg flux ratio of 16. Subsequently, 5-period $ZnO/Zn_{0.55}Mg_{0.45}O$ QWs were grown with the well width and the barrier thickness of 1.1 and 0.6 nm, respectively. A 10 nm $Zn_{0.55}Mg_{0.45}O$ cap layer was finally deposited on top of the structure. The Mg content was *ex situ* measured from an epilayer sample grown at the same Zn/Mg flux ratio (16) to be $x = 0.45$ by energy dispersive spectroscopy (EDS) in a field emission SEM operating at 3 kV. The X-ray ranges for the Zn Lα, Mg Kα and O Kα radiations obtained from simulation are 90, 90 and 100 nm, respectively, all of which are smaller than the thicknesses of the epilayers (150-300 nm).

The surface morphology, microstructure and strain relaxation conditions were characterized in our previous work [22]. Here we focus on the polarized light emission. The experimental set-up for PL measurements consists of a solid state laser DTL-389QT with an emission wavelength 263 nm used as an excitation source, a grating monochromator Andor Shamrock SR-303i-B for analysis of luminescence and a CCD camera Andor DV 420A-BU2 for detection of luminescence signal, as shown in Fig. 1. The monochromator and CCD camera are controlled by a computer. The sample is mounted in a refrigerator (CCS-100/204, Janis Research Corporation) providing stable temperatures in the 10-300 K range. Making PL polarization measurements the laser beam is oriented so that the electrical vector of laser emission is directed vertically, while a polariser inserted into the luminescence channel is oriented either vertically (at 0°) or horizontally (at 90°).

Optics EXPRESS

The DOP for each luminescence wavelength is calculated according to the formula:

$$P = (I_{90} - I_0)/(I_{90} + I_0) \times 100\%$$

where I_{90} and I_0 are the intensity of the PL emission which are measured through a polarizer oriented perpendicular and parallel to the [0001] (c) direction, respectively. Here it should be mentioned that the 263 nm light has a rather limited penetration (probing) depth. This is a major difference to unpolarized CL measurements.

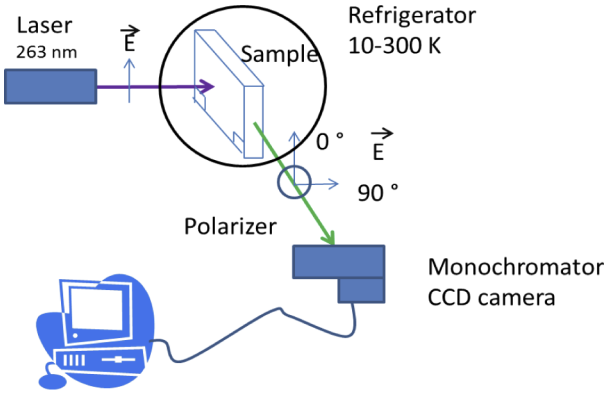

Fig. 1. Experimental set-up for polarized PL measurements.

3. Results and discussion

The PL spectra of the LGO substrate were first investigated in order to determine whether it has influence on the luminescence characteristics of the ZnO samples. Figure 2 shows the PL spectra and degree of polarization of LGO (100) in the temperature range of 10-300 K. One can observe a broad peak at approximately 1.8 eV accompanied by a weak peak at 2.4 eV, which presumably arises as a result of recombination of geminate donor-acceptor pairs [25]. The PL intensity decreases apparently with the increasing temperature. The DOP of LGO substrate was found to be around 5~25% at 1.5-3.0 eV, which is independent on the temperature. Taking into consideration the negligible PL intensity of LGO at 3.2-4.2 eV, the spectral features of the ZnO samples will not be influenced by the substrate.

Figure 3(a) shows the 90° polarized PL spectra of the m-plane ZnO epilayer at 10-300 K. A moderate emission at 3.260 eV and a strong emission at 3.221 eV with a full width at half maximum (FWHM) of 25 meV are observed at 10 K. The former corresponds to the near band edge (NBE) exciton emission (superposition of donor bound exciton D^0X and free exciton FX) [26,27], whereas the latter is a BSF related emission [20,28]. The strong BSFs related peak is the result of the high density of BSFs of 1×10^6 cm^{-1} in the epilayer reported previously [22]. As suggested, the BSFs are treated as quantum wells of a type-II band alignment [29,30]. The strong confinement effect results in the strong emission at 3.221 eV. The phonon replica of BSFs emission at 3.155 eV and 3.087 eV can also be observed. The luminescence intensities of both NBE and BSFs decrease with temperature up to 150 K and then disappear in the noise. This can be attributed to the non-radiative coupling to phonons causing bandgap shrinkage [4]. Two broad emissions at approximately 1.8 and 2.4 eV are also observed at low temperature, which are mainly contributed from the LGO substrate. The 0° polarized spectra shown in Fig. 3(b) exhibit the same feature as that of 90°. The peak position of NBE and BSFs emission is almost identical for 90° and 0° polarization in the temperature range of 10-150 K, which is different from the reported energy difference ΔE of 20~60 meV in nonpolar ZnO layers [2,5]. Figure 3(c)

Optics EXPRESS

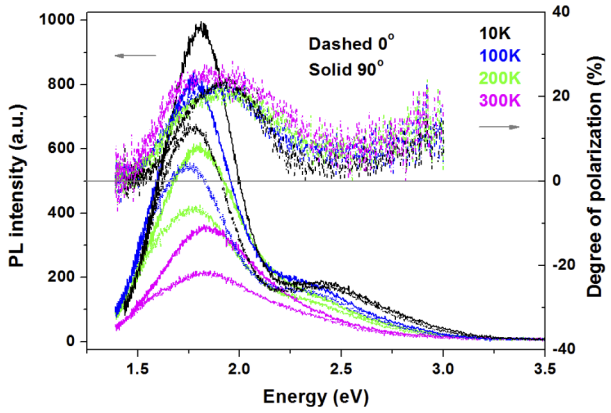

Fig. 2. Polarized PL spectra (0° and 90°) and the corresponding degree of polarization of the LGO (100) substrate in the temperature range of 10-300 K.

shows the degree of polarization of m-plane ZnO epilayer at different temperatures. The DOP decreases gradually from 30% at 10 K to 7% at 150 K for the BSF emission, whereas that of the NBE emission is as low as 10% at 10-50 K. Accordingly, the NBE emission shows a weaker polarization characteristic than the BSF one.

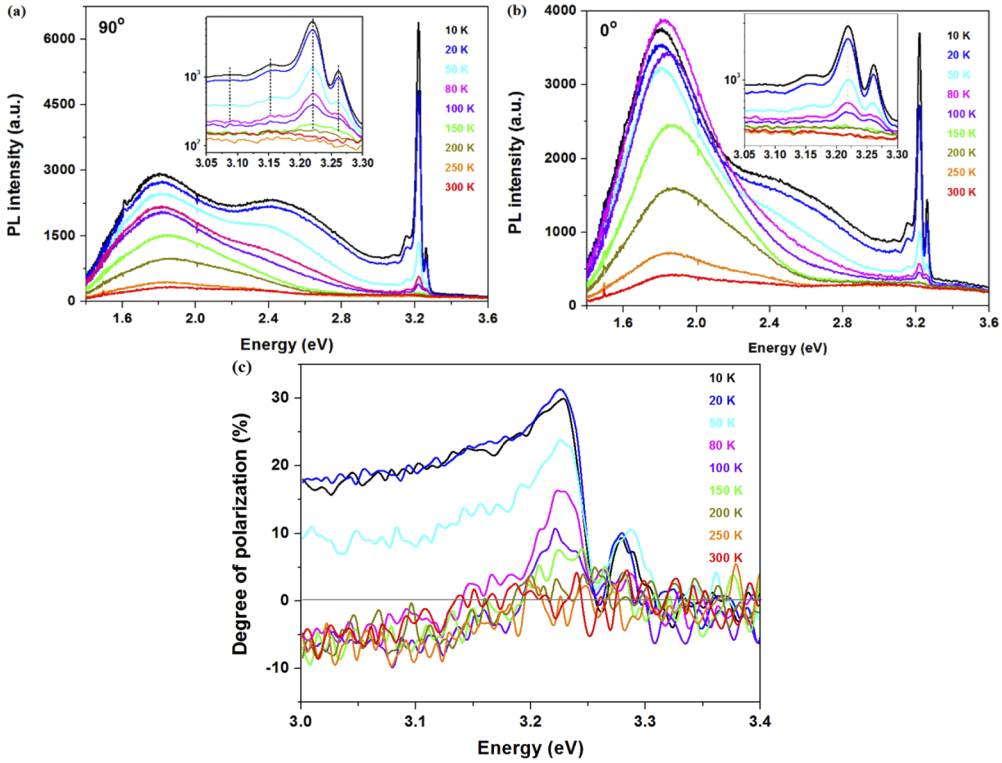

Fig. 3. (a) 90° and (b) 0° polarized PL spectra and (c) the corresponding degree of polarization of the m-plane ZnO epilayer at 10-300 K.

Optics EXPRESS

Figure 4(a) shows the polarized PL spectra of m-plane ZnO QWs recorded at 10-300 K. A strong emission at 3.625 eV with a FWHM value of ~350 meV was observed at 10 K for 90° polarization. The QWs peak shows a pronounced blue shift due to the positive quantum confinement effect and the absence of internal polarization field. The high FWHM value originates from the thin well thickness and the wavy interface [31]. The variation of degree of polarization with temperature is shown in Fig. 4(b). The DOP of the QWs emission is 66% at low temperature, which gradually decreases to 48% at room temperature. The decreasing DOP with temperature can be explained by thermal population of photo-generated carriers through phonon scattering [4]. The peak energy of the QW emission at 0° and 90° polarization are shown in Fig. 4(c) in the temperature range of 10-300 K. The peak position at 90° polarization decreases from 3.625 eV (10-100 K) to 3.536 eV (300 K), whereas the peak energy at 0° polarization increases from 3.590 eV (10 K) to 3.596 eV (50 K) and then decreases to 3.556 eV (300 K). The slight blue-red shift is usually attributed to the radiative emission of localized excitons [32,33]. The energy difference ΔE (E_{90}-E_0) between 90° and 0° polarization varies from +30 meV at low temperature to -20 meV at room temperature. The ΔE at room temperature is similar to that of reported results, but the value at low temperature differs greatly in each measurement [3,4,8]. In order to obtain a better understanding of the excitons in QWs, the quenching behaviors of the localized excitons are also investigated. The integrated intensity of the QW peak as a function of reciprocal temperature is plotted in Fig. 4(d). The plot can be well fitted by the well-known Arrhenius expression [34,35]:

$$I = I_0/(1 + a_1 \exp(-E_{a1}/kT) + a_2 \exp(-E_{a2}/kT))$$

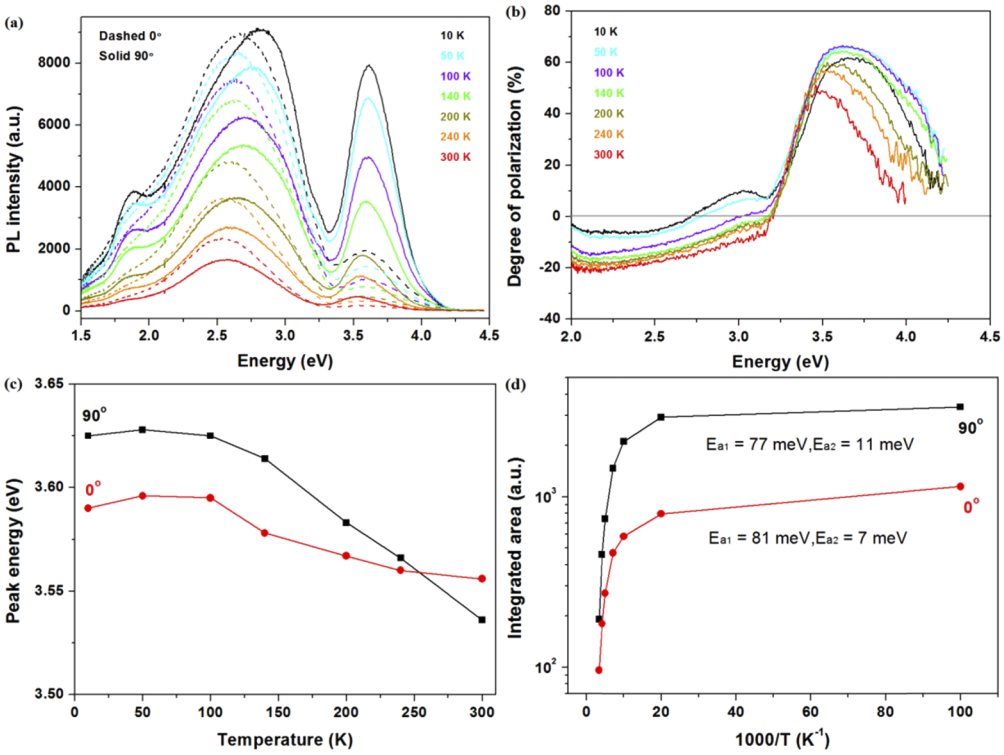

Fig. 4. (a) 0° and 90° Polarized PL spectra, (b) the corresponding degree of polarization, (c) peak energy of QWs emission versus T and (d) integrated PL intensity of QWs peak versus 1/T of the m-plane ZnO QWs at 10-300 K.

Optics EXPRESS

where I and I_0 are the intensity at temperature T and 0 K, a_1 and a_2 are the coefficients measuring the quenching efficiency, E_a is the activation energy for the thermal quenching process, and k is the Boltzmann constant. E_{a1} and E_{a2} describe the nonradiative recombination at low and high temperature. The mean values of E_{a1} and E_{a2} are found to be about 9 and 80 meV, respectively. The observation of two different activation energy values indicates that there are two competitive nonradiative recombination channels. The activation energy E_{a2} of 80 meV deduced from $ZnO/Zn_{0.55}Mg_{0.45}O$ QWs is higher than the exciton binding energy of 60 meV for bulk ZnO, which can be explained by the quantum confinement effect. As a matter of fact, the exciton binding energy is dependent on the well width and barrier height [36,37].

To further investigate whether the polarization of the laser beam has an influence on that of the QWs, the polarized PL spectra were acquired by a polarized incident laser with its electrical vector E_L oriented perpendicular and parallel to the c-axis direction, respectively. An apparent peak of QWs can be observed for $E_L \perp c$ and $E_L // c$ from 10 to 300 K, as shown in Figs. 5(a) and 5(b). The emission intensity of QWs at $E_L // c$ is 2~3 times higher than those at $E_L \perp c$. The influence of laser beam polarization on the energy difference ΔE is very similar to that induced by the polarizer. The degree of polarization at different temperatures is demonstrated in Fig. 5(c). Under the condition of $E_L // c$, the DOP of the QW emission decreases obviously from 72~76% at 10-200 K to 25% at 300 K. However, the DOP at $E_L \perp c$ increases first from 60% at 10 K to 73% at 100 K and then decreases to 42% at 300 K.

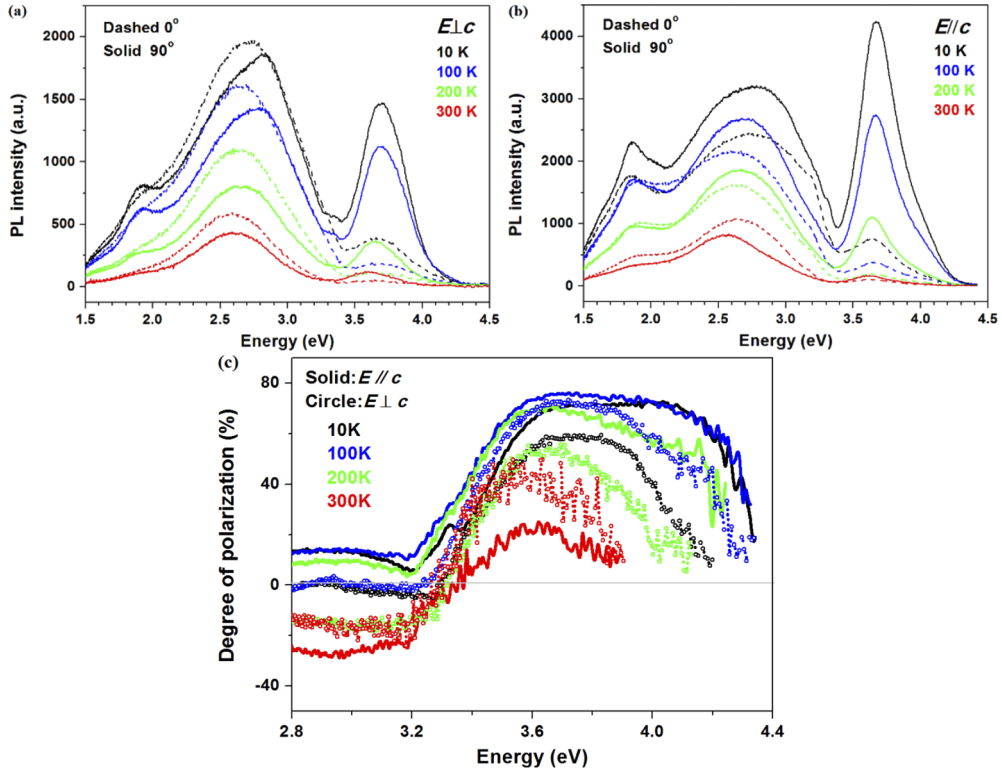

Fig. 5. 0° and 90° Polarized PL spectra generated by polarized laser light incident at (a) $E_L \perp c$ and (b) $E_L // c$ and (c) the corresponding degree of polarization of the m-plane ZnO QWs at 10-300 K.

Figure 6(a) shows the polarized spectra of the a-plane ZnO epilayer at 10-300 K. Two strong emissions at 3.240 eV and 3.320 eV are observed at low temperature, which corresponds to the

Optics EXPRESS

BSFs and NBE emission. With the temperature increasing up to 100 K, the dominant emission peak changes from BSF to NBE. The peak energy of BSFs is monotonously red-shifted from 3.240 to 3.166 eV, while that of NBE is blue-shifted from 3.320 to 3.344 eV and then red-shifted to 3.305 eV. The peak position of BSF and NBE emission in the a-ZnO epilayer are almost identical for 90° and 0° polarization in the measured temperature range, which is the same as that observed in the m-ZnO epilayer. Figure 6(b) shows the degree of polarization of the a-plane ZnO epilayer at different temperatures. The DOP of the BSF emission decreases from 42% at 10-140 K to 25% at 300 K, whereas the value for the NBE emission decreases from 74% at 10-50 K to 33% at 300 K. The NBE emission thus exhibits a higher DOP than the BSFs in the a-plane ZnO epilayer, especially at low temperature.

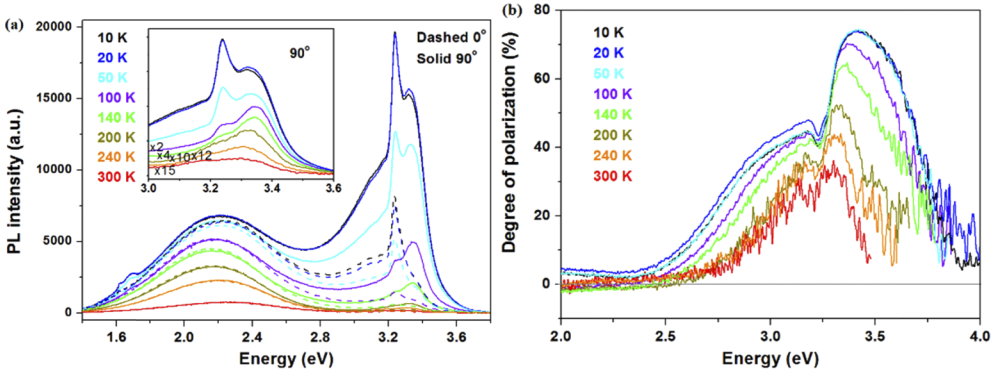

Fig. 6. (a) 0° and 90° Polarized PL spectra and (b) the corresponding degree of polarization of the a-plane ZnO epilayer at 10-300 K.

The polarization of nonpolar ZnO originates from the band splitting of the *p*-like valence bands in the wurtzite structure, which split into three subbands due to the crystal field interaction and spin orbital interaction [39]. Since the photo-excited holes occupy the states of the valence band by the Boltzmann-like distribution, the NBE intensity with $E//c$ will be lower in intensity. It is reported that the excitonic selection rules related to the electronic band structure will be modified markedly by introducing in-plane anisotropic strains. The $\boldsymbol{k \cdot p}$ perturbation theory has been employed to reveal the effect of in-plane stains on the transition energy and the oscillator strength [5,9]. Table 1 summarizes the degree of polarization, in-plane strains and ΔE value of nonpolar m- and a-plane ZnO epilayers and QWs grown on different substrates. As shown in Table 1, the nonpolar ZnO samples demonstrate a wide range of DOP from being nearly in absent to 89% at room temperature. Comparing the strain state and DOP of all the samples, one can observe that the influence of in-plane strains on the degree of polarization and ΔE is complicated and indecisive. It seems that the quantity of residual strain and the extent of strain relaxation as well as the direction of in-plane strain will affect the degree of polarization. Another observation from Table 1 is that, the DOP is low when the ΔE value is small. The phenomenological correlation between ΔE and DOP is roughly applicable for nonpolar ZnO except the samples in Ref. [16]. Although the strain state of a-ZnO epilayer is very similar ($\varepsilon_{yy} \approx 0$, ε_{zz} = -0.2~-0.7%), the DOP varies from 0.22 to 0.89. What is more confusing to us is that the DOP is largely different despite at the approximate strain state, for instance, a-plane ZnO on sapphire reported in Ref. [16] and [5]. In the present case, the m-ZnO epilayer showed moderate polarity solely for the emission generated by BSFs at low temperature. The m-ZnO QWs, however, exhibited strong polarity at the entire temperature range. We speculate that the microstructural defects in the nonpolar samples might play an important role in addition to the strain state. Various kinds of defects may be formed during the particular growth conditions on different substrates [40], which can apparently change the electronic band structure of the conduction band and valence

Optics EXPRESS

Table 1. Degree of polarization, in-plane strains and ΔE value of nonpolar m- and a-plane ZnO epilayer and QWs samples.

Sample	Substrate	Mismatch	In-plane strains	ΔE (meV)	Degree of polarization		Ref.
					300 K	10 K	
m-ZnO	ZnO		strain free	-42	49%		[8]
			ε_{xx} = -0.0004 ε_{zz} = -0.0081	-40	55%		
	$LaAlO_3$	f_{xx} = +1.0% f_{zz} = +2.8%	ε_{xx} = +0.0012 ε_{zz} = +0.0027	~0	10%		[9]
	$LiGaO_2$	f_{xx} = -1.9% f_{zz} = -3.9%	ε_{xx} = -0.0080 ε_{zz} = -0.0050	~0	4%	30% (BSF) 10% (NBE)	this work
m-QWs	ZnO		strain free	-37 -27	43% (L = 2.8) 26% (L = 1.4)	92% 81%	[8]
	$m\text{-}Al_2O_3$	f_{xx} = +75% f_{zz} = -9.4%	N/A	-29	55% (BSF) 52% (NBE)	90% (BSF) 93% (NBE)	[4]
	$LiGaO_2$	f_{xx} = -2.6% f_{zz} = -2.7%	ε_{xx} = +0.0030 ε_{zz} = -0.0230	-20	40%	76%	this work
	wafer			-37	57%		[38]
a-ZnO	ZnO		strain free	-41	51%		[2]
			ε_{yy} = -0.0004 ε_{zz} = -0.0071	-22	61%		
	GaN	f_{yy} = -1.9% f_{zz} = -0.4%	ε_{yy} = 0.0007 ε_{zz} = -0.0016	-4	89%		[16]
	$r\text{-}Al_2O_3$		ε_{yy} = 0.0019 ε_{zz} = -0.0067	-9	84%		[16]
			ε_{yy} = 0.0007 ε_{zz} = -0.0025	N/A		72%	[7]
		f_{yy} = -18% f_{zz} = -1.6%	ε_{yy} = +0.0042 ε_{zz} = -0.0061	-18	36%		[5]
			ε_{yy} = -0.0011 ε_{zz} = -0.0046	-42	70%		[5]
			N/A	N/A	63% (450 °C) 22% (600 °C)		[17]
	$LiGaO_2$	f_{yy} = -4.1% f_{zz} = -3.9%	ε_{yy} = +0.0002 ε_{zz} = -0.0040	~0	25% (BSF) 33% (NBE)	42% (BSF) 74% (NBE)	this work
a-QWs	ZnO		N/A	-20	51%	96%	[15]
			N/A	N/A	99%	99%	[3]

band. With regard to ZnO epilayer and QWs grown on LGO substrate, it has been demonstrated that the samples contained a high density of BSFs which acted as type II quantum wells and generated strong emission at an energy about 40 meV lower than that of NBE. The BSFs oriented perpendicularly to the QWs and the intersections of them might form additional one-dimension confinement structures. The high DOP of the QWs sample might therefore be attributed to the enhanced confinement effect of the one-dimension confinement structures caused by the intersection of QW and BSF. Further study is definitely needed to validate the hypothesis. The

Optics EXPRESS

DOP of nonpolar ZnO in this work is lower than those of previously reported values, which might be associated with the excitation source used here. In the present case, the PL spectra were excited by a laser with a wavelength of 263 nm. The short wavelength exhibits a rather low penetration depth of only the topmost 50-100 nm.

4. Conclusion

In summary, the polarized PL spectra of nonpolar m- and a-plane ZnO epilayers and QWs were investigated under the excitation of 263 nm solid state laser. The m-plane ZnO epilayer exhibits a weak anisotropy with the degree of polarization of 30% for BSFs and 10% for the NBE emission at 10 K, which is nearly in absent at room temperature. The degree of polarization of m-plane QWs changes from 76% at 10 K to 40% at 300 K. The strong anisotropy might be attributed to the enhanced confinement effect of a one-dimension confinement structure caused by the intersection of QW and BSF. In addition to the temperature, the degree of polarization was also influenced by the polarization of exciting laser beam. As for the a-plane ZnO epilayer, the degree of polarization of 74% for the NBE emission is higher than that of 42% for BSFs at 10 K, which decreases to 33% and 25% at 300 K, respectively.

Funding

Ministry of Science and Technology, Taiwan (104-2221-E-110-012-MY3, 107-2221-E-110-004-MY3); National Natural Science Foundation of China (51602309, U1605245).

Disclosures

The authors declare no conflicts of interest.

References

1. J. Dai, J. Chen, X. Li, J. Zhang, H. Long, H. Kuo, Y. He, and C. Chen, "Ultraviolet polarized light emitting and detecting dual-functioning device based on nonpolar n-ZnO/i-ZnO/p-AlGaN heterojunction," Opt. Lett. **44**(8), 1944 (2019).
2. H. Matsui and H. Tabata, "Lattice strains and polarized luminescence in homoepitaxial growth of a-plane ZnO," Appl. Phys. Lett. **101**(23), 231901 (2012).
3. M. J. Mohammed Ali, J. M. Chauveau, and T. Bretagnon, "Anisotropic optical properties of a homoepitaxial (Zn, Mg)O/ZnO quantum well grown on a-plane ZnO substrate," Phys. Status Solidi C **13**(7-9), 598–601 (2016).
4. H. R. Chen, C. Y. Tsai, Y. C. Huang, C. C. Kuo, H. C. Hsu, and W. F. Hsieh, "Optical properties of one- and two-dimensional excitons in m-plane ZnO/MgZnO multiple quantum wells," J. Phys. D: Appl. Phys. **49**(9), 095105 (2016).
5. H. Matsui, N. Hasuike, H. Harima, and H. Tabata, "Engineering of optical polarization based on electronic band structures of A-plane ZnO layers under biaxial strains," J. Appl. Phys. **116**(11), 113505 (2014).
6. J.-M. Chauveau, M. Teisseire, H. Kim-Chauveau, C. Morhain, C. Deparis, and B. Vinter, "Anisotropic strain effects on the photoluminescence emission from heteroepitaxial and homoepitaxial nonpolar (Zn,Mg)O/ZnO quantum wells," Appl. Phys. Lett. **109**, 102420 (2011).
7. C.-M. Lai, Y.-E. Huang, K.-Y. Kou, C.-H. Chen, L.-W. Tu, and S.-W. Feng, "Experimental and theoretical study of polarized photoluminescence caused by anisotropic strain relaxation in nonpolar a-plane textured ZnO grown by a low-pressure chemical vapor deposition," Appl. Phys. Lett. **107**(2), 022110 (2015).
8. H. Matsui and H. Tabata, "In-plane anisotropy of polarized photoluminescence in M-plane (10-10) ZnO and MgZnO/ZnO multiple quantum wells," Appl. Phys. Lett. **94**(16), 161907 (2009).
9. H. H. Wang, J. S. Tian, C. Y. Chen, H. H. Huang, Y. C. Yeh, P. Y. Deng, L. Chang, Y. H. Chu, Y. R. Wu, and J. H. He, "The effect of tensile strain on optical anisotropy and exciton of m-plane ZnO," IEEE Photonics J. **7**, 6800708 (2015).
10. C.-Y. Chen, J.-H. Huang, K.-Y. Lai, Y.-J. Jen, C.-P. Liu, and J.-H. He, "Giant optical anisotropy of oblique-aligned ZnO nanowire arrays," Opt. Express **20**(3), 2015 (2012).
11. G. Tabares, A. Hierro, B. Vinter, and J.-M. Chauveau, "Polarization-sensitive Schottky photodiodes based on a-plane ZnO/ZnMgO multiple quantum-wells," Appl. Phys. Lett. **99**(7), 071108 (2011).
12. J. Gao, Y. Zhang, Y. Sun, and Q. Wu, "Ultra-wide band and multifunctional polarization converter based on dielectric metamaterial," Materials **12**(23), 3857 (2019).
13. S. Jiang, S. Gholam-Mirzaei, E. Crites, J. E. Beetar, M. Singh, R. Lu, M. Chini, and C. D. Lin, "Crystal symmetry and polarization of high-order harmonics in ZnO," J. Phys. B: At., Mol. Opt. Phys. **52**(22), 225601 (2019).

Optics EXPRESS

14. P. Shankar and J. B. B. Rayappan, "Room temperature ethanol sensing properties of ZnO nanorods prepared using an electrospinning technique," J. Mater. Chem. C **5**(41), 10869–10880 (2017).
15. D.-R. Hang, S. E. Islam, K. H. Sharma, C. Chen, C.-T. Liang, and M. M. C. Chou, "Optical characteristics of nonpolar a-plane ZnO thin film on (010) LiGaO2 substrate," Semicond. Sci. Technol. **29**(8), 085004 (2014).
16. J. Chen, J. Zhang, J. Dai, F. Wu, S. Wang, H. Long, R. Liang, J. Xu, C. Chen, Z. Tang, Y. He, M. Li, and Z. Feng, "Strain dependent anisotropy in photoluminescence of heteroepitaxial nonpolar a-plane ZnO layers," Opt. Mater. Express **7**(11), 3944 (2017).
17. A. Kato, S. One, M. Ikeda, R. Tajima, Y. Adachi, and K. Yasui, "Polarization properties of nonpolar ZnO films grown on R-sapphire substrates using high-temperature H2O generated by a catalytic reaction," Thin Solid Films **644**, 29–32 (2017).
18. D. Gerthsen, D. Litvinov, T. Gruber, C. Kirchner, and A. Waag, "Origin and consequences of a high stacking fault density in epitaxial ZnO layers," Appl. Phys. Lett. **81**(21), 3972–3974 (2002).
19. A. Ievtushenko, V. Karpyna, J. Eriksson, I. Tsiaoussis, I. Shtepliuk, G. Lashkarev, R. Yakimova, and V. Khranovskyy, "Effect of Ag doping on the structural, electrical and optical properties of ZnO grown by MOCVD at different substrate temperatures," Superlattices Microstruct. **117**, 121–131 (2018).
20. W.-H. Lin, U. Jahn, H. T. Grahn, L. Chang, M. M. C. Chou, and J.-J. Wu, "Spectral and spatial luminescence distribution of m-plane ZnO epitaxial films containing stacking faults: A cathodoluminescence study," Appl. Phys. Express **6**(6), 061101 (2013).
21. J. W. Lee, J.-H. Kim, S. K. Han, S.-K. Hong, J. Y. Lee, S. I. Hong, and T. Yao, "Interface and defect structures in ZnO films on m-plane sapphire substrates," J. Cryst. Growth **312**(2), 238–244 (2010).
22. T. Yan, C.-Y. J. Lu, L. Chang, M. M. C. Chou, K. H. Ploog, C.-M. Chiang, and N. Ye, "Epitaxial growth of nonpolar m-plane ZnO epilayers and ZnO/$Zn_{0.55}Mg_{0.45}O$ multiple quantum wells on a $LiGaO_2$ (100) substrate," RSC Adv. **5**(127), 104798–104805 (2015).
23. M. M. C. Chou, D.-R. Hang, C. L. Chen, and Y.-H. Liao, "Epitaxial growth of nonpolar m-plane ZnO (10-10) on large-size $LiGaO_2$ (100) substrates," Thin Solid Films **519**(11), 3627–3631 (2011).
24. T. Huang, S. Zhou, H. Teng, H. Lin, J. Wang, P. Han, and R. Zhang, "Growth and characterization of ZnO films on (001), (100) and (010) $LiGaO_2$ substrates," J. Cryst. Growth **310**(13), 3144–3148 (2008).
25. L. Trinkler, A. Trukhin, B. Berzina, V. Korsaks, P. Ščajev, R. Nedzinskas, S. Tumėnas, and M. M. C. Chou, "Luminescence properties of $LiGaO_2$ crystal," Opt. Mater. **69**, 449–459 (2017).
26. F. Xian, G. Zheng, L. Xu, W. Kuang, S. Pei, Z. Cao, J. Li, and M. Lai, "Temperature and excitation power dependence of photoluminescence of ZnO nanorods synthesized by pattern assisted hydrothermal method," J. Alloys Compd. **710**, 695–701 (2017).
27. E. Przezdziecka, E. Guziewicz, and B. S. Witkowski, "Photoluminescence investigation of the carrier recombination processes in N-doped and undoped ZnO ALD films grown at low temperature," J. Lumin. **198**, 68–76 (2018).
28. T.-H. Huang, W.-H. Lin, T. Yan, J.-J. Wu, L. Chang, M. M. C. Chou, U. Jahn, and K. H. Ploog, "Strain relaxation, defects and cathodoluminescence of m-plane ZnO and $Zn_{0.8}Mg_{0.2}O$ epilayers grown on γ-$LiAlO_2$ substrate," ECS J. Solid State Sci. Technol. **2**, P338 (2013).
29. Y. Yan, G. M. Dalpian, M. M. Al-Jassim, and S.-H. Wei, "Energetics and electronic structure of stacking faults in ZnO," Phys. Rev. B **70**(19), 193206 (2004).
30. V. Khranovskyy, M. Sendova, B. Hosterman, N. McGinnis, I. Shtepliuk, and R. Yakimova, "Temperature dependent study of basal plane stacking faults in Ag:ZnO nanorods by Raman and photoluminescence spectroscopy," Mater. Sci. Semicond. Process. **69**, 62–67 (2017).
31. I. Gorczyca, K. Skrobas, N. E. Christensen, J. Sajkowski, M. Stachowicz, H. Teisseyre, and A. Kozanecki, "ZnO/(Zn)MgO polar and nonpolar superlattices," J. Appl. Phys. **125**(13), 135702 (2019).
32. X. Q. Gu, H. P. He, L. P. Zhu, Z. Z. Ye, K. F. Huo, and P. K. Chu, "Dependence of photoluminescence of ZnO/$Zn_{0.85}Mg_{0.15}O$ multi-quantum wells on barrier width," Phys. Lett. A **373**(36), 3281–3284 (2009).
33. M. Al-Suleiman, A. El-Shaer, A. Bakin, H. H. Wehmann, and A. Waag, "Optical investigations and exciton localization in high quality $Zn_{1-x}Mg_xO$/ZnO single quantum wells," Appl. Phys. Lett. **91**(8), 081911 (2007).
34. D. Xu, P. Zapol, G. B. Stephenson, and C. Thompson, "Kinetic Monte Carlo simulations of GaN homoepitaxy on c-and m-plane surfaces," J. Chem. Phys. **146**(14), 144702 (2017).
35. T. Zhou and Z. Zhong, "Optical properties demonstrating strong coupling of compactly arranged Ge quantum dots," Opt. Express **27**(16), 22173 (2019).
36. G. Coli and K. K. Bajaj, "Excitonic transitions in ZnO/MgZnO quantum well heterostructures," Appl. Phys. Lett. **78**(19), 2861–2863 (2001).
37. T. S. Ko, T. C. Lu, L. F. Zhuo, W. L. Wang, M. H. Liang, H. C. Kuo, S. C. Wang, L. Chang, and D. Y. Lin, "Optical characteristics of a-plane ZnO/$Zn_{0.8}Mg_{0.2}O$ multiple quantum wells grown by pulsed laser deposition," J. Appl. Phys. **108**(7), 073504 (2010).
38. B.-H. Lin, Y.-C. Wu, H.-Y. Chen, S.-C. Tseng, J.-X. Wu, X.-Y. Li, B.-Y. Chen, C.-Y. Lee, G.-C. Yin, S.-H. Chang, M.-T. Tang, and W.-F. Hsieh, "Peculiar near-band-edge emission of polarization-dependent XEOL from a non-polar a-plane ZnO wafer," Opt. Express **26**(3), 2731 (2018).
39. D. C. Reynolds, D. C. Look, B. Jogai, C. W. Litton, G. Cantwell, and W. C. Harsch, "Valence-band ordering of ZnO," Phys. Rev. B **60**(4), 2340–2344 (1999).
40. Y. Zhang, F. Qin, J. Zhu, X. Chen, J. Li, D. Tang, Y. Yang, F. Ren, C. Xu, S. Gu, R. Zhang, Y. Zheng, and J. Ye, "Low-threshold ultraviolet stimulated emissions from large-sized single crystalline ZnO transferable membranes," Opt. Express **26**(24), 31965 (2018).